*Pharmaceutical Research, Vol. 22, No. 9, September 2005 (© 2005)*
DOI: 10.1007/s11095-005-6157-8

*Research Paper*

# $^{99m}$Tc-EC-Guanine: Synthesis, Biodistribution, and Tumor Imaging in Animals

**David J. Yang,[1,2,3] Kaoru Ozaki,[1] Chang-Sok Oh,[1] Ali Azhdarinia,[1] Thomas Yang,[1] Megumi Ito,[1] Allison Greenwell,[1] Jerry Bryant,[1] Saady Kohanim,[1] Vincenzo K. Wong,[1] and E. Edmund Kim[1]**

*Received February 23, 2005; accepted May 26, 2005*

***Purpose.*** DNA markers are useful in assessing cell proliferation. The purpose of this study was to synthesize $^{99m}$Tc-ethylenedicysteine-guanine (EC-Guan) for evaluation of cell proliferation.
***Methods.*** Tumor cells were incubated with $^{99m}$Tc-EC-Guan for cell cycle analysis. Prostate tumor cells that were overexpressing the HSV thymidine kinase gene, or various tumor cells were incubated with $^{99m}$Tc-EC-Guan at 0.5–2 h. Thymidine incorporation assays were performed in lung cancer cells incubated with EC-Guan at 0.1–1 mg/well. Tissue distribution, autoradiography, and planar scintigraphy of $^{99m}$Tc-EC-Guan and $^{99m}$Tc-EC (control) were determined in tumor-bearing rodents at 0.5–4 h.
***Results.*** Cell culture assays indicated that EC-Guan was incorporated in DNA, and there was no significant uptake difference between HSVTK overexpressed and normal groups. Biodistribution and scintigraphic imaging studies of $^{99m}$Tc-EC-Guan showed increased tumor/tissue count density ratios as a function of time.
***Conclusions.*** Our results indicate that $^{99m}$Tc-EC-Guan may be useful as a tumor proliferation imaging agent.

**KEY WORDS:** biodistribution; EC-Guan; proliferation; SPECT.

## INTRODUCTION

Assessment of tumor cell proliferation by positron emission tomography (PET) and single photon emission computed tomography (SPECT) could be helpful in the evaluation of tumor growth potential, the degree of malignancy, and could provide an early assessment of treatment response (1). Several attempts have been made to assess tumor proliferative activity. It has been reported that 2′-fluorodeoxyglucose ([$^{18}$F]FDG) uptake is an indicator of tumor proliferative activity (2). Higashi *et al.* (3) have shown that [$^{18}$F]FDG uptake is strongly related to the number of viable cells. Another approach was to use a radiolabeled amino acid as a tumor cell proliferative marker (4,5). However, the structures of these agents are not purine- or pyrimidine-based, which are essential building blocks of DNA. Although several radiolabeled pyrimidine and purine have been developed, they were used as probes for imaging herpes virus type 1 thymidine kinase (HSV1-tk) expression and other reporter genes. For example, pyrimidine nucleoside [e.g., 2′-fluoro-2′-deoxy-5-iodo-1-β-D-arabinofuranosyluracil (FIAU); 2′-fluoro-2′-deoxy-5-iodo-1-β-D-ribofuranosyl-uracil (FIRU); 2′-fluoro-2′-5-methyl-1-β-D-arabinofuranosyluracil (FMAU); 2′-fluoro-2′-deoxy-5-iodovinyl-1-β-D-ribofuranosyluracil (IVFRU)] and acycloguanosine 9-[(2-hydroxy-1-(hydroxy-methyl)ethoxy)methyl]guanine (GCV) and 9-[4-hydroxy-3- (hydroxy-methyl)butyl]guanine (PCV) (6) and other $^{18}$F-labeled acycloguanosine analogs (FGCV, FPCV, FHPG, FHBG) (7–10) have been developed as reporter substrates for imaging wild-type and mutant HSV1-tk expression. It has been reported that thymidine kinase activity of pyrimidine analogs was linked to G1 and S-phase of cell cycle progression (11). HSV1-tk phosphorylates $^{18}$F-labeled acycloguanosine analogs ([$^{18}$F]GCV, [$^{18}$F]PCV, [$^{18}$F]FHBG, FIAU). The expression of these reporter genes can be linked to the expression of a therapeutic transgene and then, using PET, can be used to track the expression of the therapeutic transgene in living subjects. The difficulty with these probes is that HSV1-tk enzyme expression depends on HSV1-tk gene transduction with adenoviral vectors. The level and activity of HSV1-tk enzyme expression are likely to be altered in different transduced cells and tissue; thus, the application of HSV1-tk probe is limited.

To overcome the sensitivity of HSV1-tk enzyme expression, it would be advantageous to develop a novel tracer that interacts with endogenous thymidine kinase, subsequently targeting S-phase of the cell cycle. Such an agent would be useful in assessing the efficacy of tumor therapy by measuring proliferative activity. Synthesis and biological activity of labeled thymidine or uridine, which were incorporated into DNA/RNA, have been reported (12–14). However, either the

[1] Division of Diagnostic Imaging, The University of Texas MD Anderson Cancer Center, 1515 Holcombe Boulevard, Houston, Texas 77030, USA.
[2] Department of Experimental Diagnostic Imaging, The University of Texas MD Anderson Cancer Center, 1515 Holcombe Boulevard, Houston, Texas 77030, USA.
[3] To whom correspondence should be addressed. (e-mail: dyang@di.mdacc.tmc.edu)

**ABBREVIATIONS:** EC, ethylenedicysteine; FDG, Fluorodeoxyglucose; FLT, Fluoro-L thymidine; Guan, guanine; PET, positron emission tomography; SPECT, single photon emission computed tomography; Tk, thymidine kinase.

complex chemistry, shorter half-life of radioisotope, or stability of the agent was involved that limited their practical uses. We have previously reported that $^{18}$F-labeled adenosine, a purine analog, could measure proliferative activity by PET (15). Because of cyclotron availability and the cost of producing K$^{18}$F for PET, we have also explored the possibility of using generator-produced isotopes. $^{99m}$Tc is preferred for labeling radiopharmaceuticals because of its favorable low energy, inexpensive isotope cost, and efficient chemistry.

Several $^{99m}$Tc-labeling techniques have been reported such as $N_4$ (e.g., DOTA), $N_3S$ (e.g., MAG-3), $N_2S_2$ (e.g., ECD), $NS_3$, $S_4$ (e.g., sulfur colloid), diethylenetriamine pentaacetic acid (DTPA), $O_2S_2$ (e.g., DMSA), and hydrazinenicotinamide (HYNIC) (17–19). The nitrogen-and-sulfur combination was shown to be a stable chelator for $^{99m}$Tc-bis-aminoethanethiol tetradentate ligands, also called diaminodithiol compounds, which are known to form very stable Tc(V)O complexes on the basis of efficient binding of the oxotechnetium group to two thiol and two amine nitrogen atoms. $^{99m}$Tc-L,L-ethylenedicysteine ($^{99m}$Tc-EC) is the most successful example of $N_2S_2$ chelates. Ethylenedicysteine can be labeled with $^{99m}$Tc easily and efficiently with high radiochemical purity and stability. In addition, EC can also be labeled with $^{68}$Ga for PET imaging, and $^{68}$Ga can be obtained from a $^{68}$Ge/$^{68}$Ga generator (20).

To continuously explore other purine-based analogs using chelation radiochemistry, we synthesized a guanine analog using EC as a chelator. In this report, the synthesis and assessment of tumor growth using $^{99m}$Tc-EC-guanine (EC-Guan) were evaluated.

## MATERIALS AND METHODS

### Chemicals and Analysis

Mass spectral analyses were conducted at the University of Texas Health Science Center (Houston, TX, USA). The mass data were obtained by fast atom bombardment on a Kratos MS 50 instrument (Kratos Instrument, Ltd., Manchester, UK). $^1$H NMR and $^{13}$C NMR studies were performed on Bruker 300 MHz spectrometer at the NMR core facility at MD Anderson Cancer Center (Houston, TX, USA). *N*-Hydroxysulfosuccinimide (Sulfo-NHS) and 1-ethyl-3-(3-dimethylaminopropyl) carbodiimide-HCl (EDAC) were purchased from Pierce Chemical (Rockford, IL, USA). 9-[4-Hydroxy-3-(hydroxymethyl)butyl]guanine (penciclovir) was purchased from LKT Laboratories (St. Paul, MN, USA). All other chemicals were purchased from Aldrich (Milwaukee, WI, USA). Silica gel coated thin-layer chromatography (TLC) plates were purchased from Whatman (Clifton, NJ, USA).

### Synthesis of 9-[4-amino-3-(hydroxymethyl)butyl]guanine (Guan, compound I)

$N^2$-(*p*-anisyldiphenylmethyl)-9-[(4-tosyl)-3-*p*-anisyldiphenylmethoxymethylbutyl]guanine (500 mg, 0.52 mmol, exact mass $C_{57}H_{54}N_5O_5S$ (M + H)$^+$ 952.37) (10) was dissolved in *N*,*N*-dimethylformamide (15 mL) and sodium azide (160 mg, 2.5 mmol) was added. The reaction mixture was heated at 100°C for 2 h with stirring. The mixture was cooled to room temperature and evaporated under reduced pressure to reduce to 1/4 of the solvent volume. Ethyl acetate (30 mL) and water (25 mL) were added to the residue, and the mixture was agitated. Next, the water layer was extracted with ethyl acetate (2 × 30 mL). Then the solvent mixture was washed with distilled water (2 × 25 mL). The gathered solvent layer was dried over magnesium sulfate (anhydrous). After filtration, the solvent was evaporated to dryness, the desired azido compound weighed 453 mg. $^1$H NMR ($CDCl_3$): $\delta$ 8.04 (s, 1H), 7.22–7.45 (m, 20H), 6.86 (d, 4H, $J$ = 9.0 Hz), 6.78 (d, 4H, $J$ = 9.0 Hz), 3.79 (s, 3H), 3.76 (s, 3H), 3.55–3.65 (m, 2H), 3.25–3.35 (m, 2H), 1.63–1.73 (m, 2H), 1.32–1.42 (m, 1H), 1.16 (d, 2H, $J$ = 3.6 Hz). Exact mass calculated for $C_{50}H_{46}N_8O_4$ (M + H)$^+$ 823.36 found 823.4.

The crude azido compound (453 mg) was dissolved in dried tetrahydrofuran (30 mL) and triphenylphosphine (655 mg, 2.5 mmol) was added. The reaction mixture was stirred at room temperature overnight. Hydrochloric acid (HCl 5 N, 1 mL) was added to the solution and the mixture was heated under reflux for 5 h. The reaction mixture was filtered and the solution was evaporated to dryness. The residue was mixed with water (25 mL) and washed with ethyl acetate (2 × 25 mL). The pH was adjusted to 7–8 by adding sodium hydroxide (1 N), and the product solution was isolated a through the column chromatography using Sephadex-G15 as a packing material. After freeze-drying (Labconco, Kansas City, MO, USA), compound **I** was obtained (100 mg, 76.2% yield). Ninhydrin (2% in methanol) spray test showed the presence of amino group. $^1$H NMR ($CDCl_3$): $\delta$ 7.60 (s, 1H), 3.98 (t, 2H, $J$ = 7.2 Hz), 3.46–3.61 (m, 2H), 2.90 (d, 2H, $J$ = 6.0 Hz), 1.72 (m, 2H), 1.43 (m, 1H). FAB MS: 253 (M + H)$^+$.

### Synthesis of $^{99m}$Tc-ethylenedicysteine-9-[4-amino-3-(hydroxymethyl)butyl] guanine conjugate ($^{99m}$Tc-EC-Guan)

Ethylenedicysteine (EC) was conjugated to Guan according to the established method using water-soluble carbodiimide as a coupling agent. The general process was described in our previous reports (21–28). Briefly, sodium hydroxide (1 N, 0.2 mL) and sodium bicarbonate (1 N, 0.2 mL) were added to a stirred solution of EC (50 mg, 0.19 mmol, m.p. 253°C, reported 251–253°C) in water (5 mL). To this colorless solution, sulfo-NHS (95.5 mg, 0.44 mmol), EDAC (84.5 mg, 0.44 mmol), and compound I (50 mg, 0.20 mmol) were added. The mixture was stirred at room temperature overnight. The mixture was dialyzed for 24 h using Spectra/POR dialysis membrane with molecule cut-off at 500 (Spectrum Medical Industries, Houston, TX, USA). After dialysis, the product was freeze-dried to afford EC-Guan (50 mg, 0.08 mmol, yield 40%). $^1$H NMR ($CDCl_3$): $\delta$ 8.04 (s, 1H), 7.22–7.45 (m, 20H), 6.86 (d, 4H, $J$ = 9.0 Hz), 6.78 (d, 4H, $J$ = 9.0 Hz), 3.79 (s, 3H), 3.76 (s, 3H), 3.55–3.65 (m, 2H), 3.25–3.35 (m, 2H), 1.63–1.73 (m, 2H), 1.32–1.42 (m, 1H), 1.16 (d, 2H, $J$ = 3.6 Hz). FAB MS: 569 (M + H)$^+$. Exact mass calculated for $C_{18}H_{27}N_8Na_3O_5S_2$ (M + H)$^+$ 568.56 found 568.93. The synthetic scheme is shown in Fig. 1.

Eethylenedicysteine-Guan (5 mg) was dissolved in 0.2 mL water. Tin (II) chloride solution (0.1 mL, 1 mg/mL) was added. Sodium pertechnetate ($Na^{99m}TcO_4$, 37–370

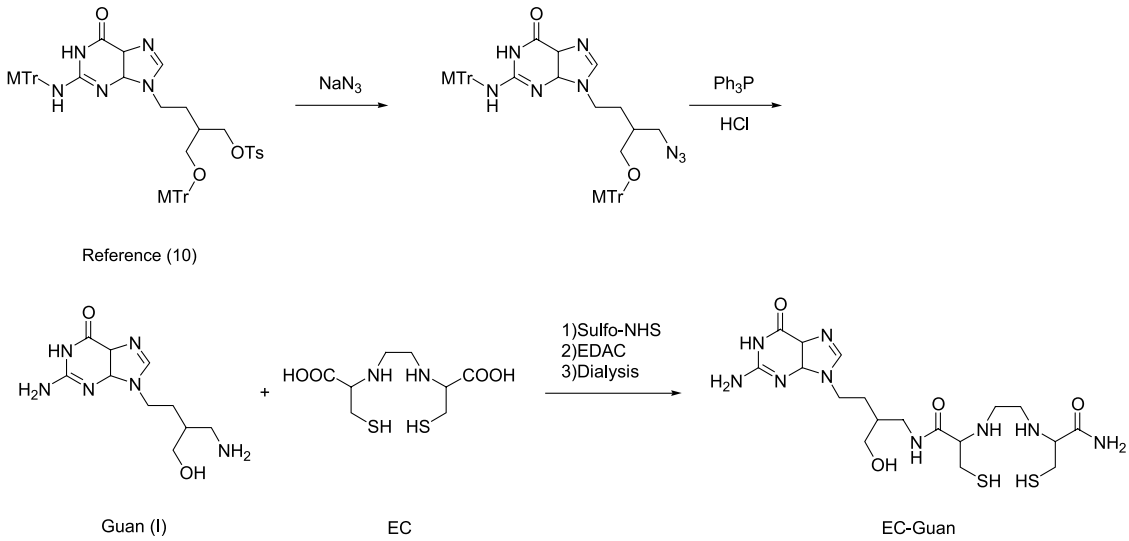


**Fig. 1.** $^{99m}$Tc-EC-Guan was synthesized by reacting aminoguanine analog (I) and ethylenedicysteine (EC) in the presence of coupling agents, followed by tin (II) chloride and pertechnetate.

MBq; Mallinckrodt, Houston, TX, USA) was added. Finally, water was added to this solution to adjust the volume to 1 mL. Radiochemical purity was assessed by radio-TLC (ITLC SG; Gelman Sciences, Ann Arbor, MI, USA) using 1 M ammonium acetate/methanol (4:1) as an eluant.

### Cell Cycle Uptake Assays

Human lung cancer cells (20 million, adherent) were cultured in RPMI in T75 flasks. The cells were washed with phosphate-buffered saline (PBS) twice and serum-free media was added. A 5-μL portion of Hoechst 33342 (2′-(4-ethoxyphenyl)-5-(4-methyl-1-peperazinyl)-2,5′-bi-1*H*-benzimidazole, stock solution: 1 mg/mL) was added per 1 mL of RPMI. The cells were incubated at 37°C for 90 min. The media was aspirated and washed with PBS. The cells were trypsinized and collected in a 15-mL test tube. The cells were sorted using a fluorescence activated cell sorter (FACS). The cells were plated to a 12-well tissue culture plate containing 50,000 cells/well and it was incubated for 24 h. To each group consisting of three wells, 4 μCi (0.148 MBq) of $^{99m}$Tc-EC-Guan or $^{99m}$Tc-EC was added. After incubation at 0.5–4 h, cells were washed with ice-cold PBS twice and trypsinized with 0.5 mL of trypsin solution. Next, cells were collected, and radioactivity, which was incorporated into cells, was measured by gamma counter (Packard Instrument, Downers Grove, IL). Data are expressed in mean ± SD percent uptake ratio.

### [$^3$H]Thymidine Incorporation Assay

To demonstrate whether EC-Guan interacts with endogenous thymidine kinase and subsequently measuring the proliferative activity of the cell cycle, a thymidine incorporation assay was performed. Fluorodeoxyglucose was selected as control because it is a gold standard for PET. Human lung tumor cells (A549) were plated at 50,000 cells/well in 200 μL RPMI, 10%FCS. EC-Guan, FDG, and D-glucose (0.1–1 mg/well) and saline (control) were added to this 96-well culture plate and incubated in 5% $CO_2$/air at 37°C. After 24 h, each well was pulsed with 0.5 μCi/10 μL [$^3$H]thymidine and incubated for 24 h. Cells were then harvested, trypsinized with 100 μL of trypsin, and incubated for 10 min in the incubator. Cells were counted using a Beckman LS380 liquid scintillation counter. Cellular uptake of [$^3$H]thymidine in the control group was unified to be 100 (baseline).

### *In Vitro* Cellular Uptake of $^{99m}$Tc-EC-Guan

To determine whether $^{99m}$Tc-EC-Guan was a broad marker for assessment of tumor growth, three different human cancer cell lines (lung NSCLC A549, ovarian OCA3, and prostate PC-3) were selected for cellular uptake assays. To determine the amount of cellular uptake at early time intervals, shorter time intervals (30 min) were included in all three-cell lines as a standard. Longer and immediate time intervals were only included in some of the cell lines for comparison to 30-min intervals. The cell lines were obtained from American Type Culture Collection (Rockville, MD). The cells were plated to a 12-well tissue culture plate containing 50,000 cells/well. To each well, 4 μCi (0.148 MBq) of $^{99m}$Tc-EC-Guan or $^{99m}$Tc-EC (0.1 mg/well) was added. Cells were incubated with radiotracers at 37°C at different time intervals. To demonstrate whether the cellular uptake of $^{99m}$Tc-EC-Guan was independent from herpes simplex virus type 1 thymidine kinase (HSV-TK) gene-mediated process, prostate tumor cells were transfected with the adeno-associated virus vector at an input multiplicity of 50 particles/cell containing HSV-tk gene and beta-galactosidase gene (beta-Gal, control). After incubation, cells were washed with ice-cold PBS twice and trypsinized with 0.5 nbsp;mL of trypsin solution. Then cells were collected and the radioactivity was measured by gamma counter. Data was expressed in mean ± SD percent uptake ratio of three measurements.

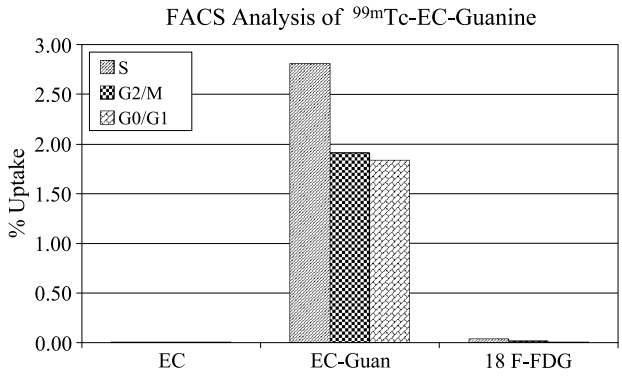


**Fig. 2.** Cell cycle phases were sorted by fluorescence activated cell sorter. Cell cycle uptake assays using lung tumor cells indicated that high uptake of $^{99m}$Tc-EC-Guan was observed in cell cycle S-phase, whereas $^{18}$F-FDG had poor uptake.

### Biodistribution and Dosimetry of $^{99m}$Tc-EC-Guan in Tumor-bearing Rats

The animals were housed in The University of Texas M. D. Anderson Cancer Center facility. All protocols involving animals [rats and rabbits (see below)] were approved by the M. D. Anderson Animal Use and Care Committee. Fischer-344 rats (150 ± 25 g) (Harlan Sprague–Dawley, Indianapolis, IN USA) ($n$ = 18) were inoculated subcutaneously with rat breast adenocarcinoma cells ($10^6$ cells/rodent) into the lumber region in legs using 25-gauge needles. The studies were performed 12–15 days after inoculation. Tumor sizes of approximately 1 cm were measured. Separate biodistribution studies using $^{99m}$Tc-EC-Guan (Study 1, nine rats) and $^{99m}$Tc-EC (Study 2, nine rats) were conducted. For each compound, the rodents were divided into three groups for three time intervals (0.5, 2, and 4 h, $n$ = 3/time point). The injection activity was 25 ± 0.5 μCi (0.925 ± 0.019 MBq) / rat. The injected mass of $^{99m}$Tc-EC-Guan was 0.1 mg/rodent. After the administration of radiotracers, the rats were sacrificed, and the selected tissues were excised, weighed, and counted for radioactivity. The biodistribution of tracer in each sample was calculated as a percentage of the injected dose per gram of tissue wet weight (%ID/g). Tumor/nontarget tissue count density ratios were calculated from the corresponding %ID/g values.

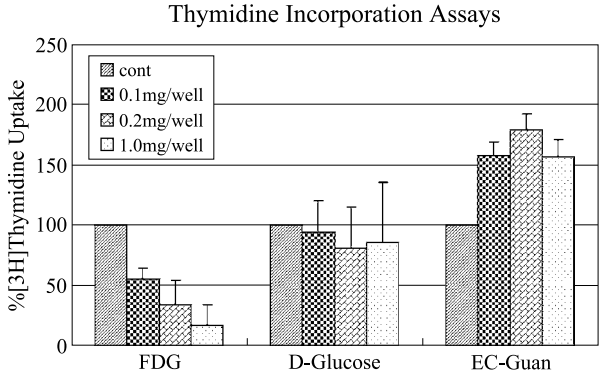


**Fig. 3.** Thymidine incorporation assays were conducted in lung cancer cells. The data showed that EC-Guan was involved in cellular proliferation. Fluorodeoxyglucose showed a dose-dependent behavior and had less involvement in cell nuclei activity.

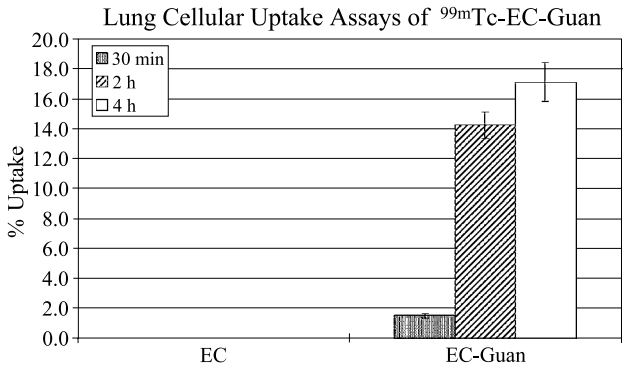


**Fig. 4.** *In vitro* cellular uptake using lung cancer cells showed that there was a markedly increased uptake of $^{99m}$Tc-EC-Guan as a function of time compared to $^{99m}$Tc-EC control groups. Data are reported as mean ± SEM ($n$ = 3). The data points were calculated as percentage of uptake.

### Planar Scintigraphic Imaging

Female New Zealand rabbits (2–3 kg) were inoculated intramuscularly with VX2 squamous carcinoma cells into the hind thigh region in legs using 25-gauge needles. Imaging studies were performed 12–15 days after inoculation. Tumor sizes of approximately 1–1.5 cm were measured. Each New Zealand rabbit was placed in a supine position and anesthetized with ketamine (50 mg/kg, i.m.), xylazine (3 mg/kg, i.m.), and acepromazine (1 mg/kg, s.c.). The supplemental dose used was ketamine (10 mg/kg, i.m.) and xylazine (0.8 mg/kg, i.m.). Planar scintigraphy was acquired for 500 k counts at immediate, 0.5–4 h after intravenous injection of $^{99m}$Tc-EC-Guan ($n$ = 3) or $^{99m}$Tc-EC (1 mCi/rabbit; 2 mg mass/rabbit, $n$ = 3). To compare the radiotracer accumulation, regions of interest (ROIs in counts per pixel) were determined. The ROIs count between tumor and muscle was used to calculate tumor/nontumor ratios.

Scintigraphic images were obtained using a M-camera from Siemens Medical Systems (Hoffman Estates, IL, USA). The camera was equipped with a low-energy parallel-hole collimator. The field of view was 53.3 × 38.7 cm. The intrinsic spatial resolution was 3.2 mm and the pixel size was 19.18 mm (32 × 32, zoom = 1) to 0.187 mm (1,024 × 1,024, zoom = 3.2). With a low-energy, high-resolution collimator (as required with $^{99m}$Tc), the system has a resultant sensitivity of 172 counts/min (cpm)/μCi and spatial resolution of 4 mm.

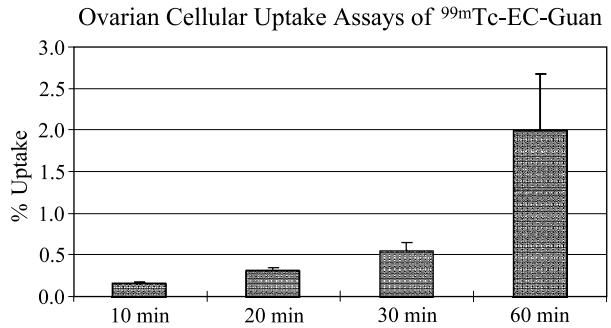


**Fig. 5.** *In vitro* cellular uptake using ovarian cancer cells showed that an increased uptake of $^{99m}$Tc-EC-Guan as a function of incubation time was observed. Data are reported as mean ± SEM ($n$ = 3).

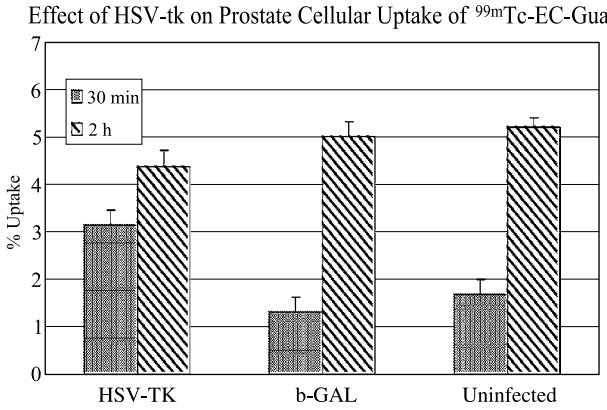


**Fig. 6.** *In vitro* cellular uptake using prostate cancer cells showed that there were no differences among HSV-tk gene, b-gal gene, and uninfected groups at 2 h incubation. The data indicate that $^{99m}$Tc-EC-Guan, a cell cycle specific and an HSV-tk gene independent marker, could assess cellular proliferation.

### Autoradiography

Whole-body autoradiography was performed using female ovarian tumor-bearing nude mice. When the tumor reached 8 mm, tumor-bearing mice were treated with saline ($n = 3$) and paclitaxel at (60 mg/kg, single dose, $n = 3$, i.v.). To demonstrate whether $^{99m}$Tc-EC-Guan could assess tumor growth after chemotherapy, a similar tumor volume (8 mm) at baseline was selected. After pretreatment and 4 days posttreatment with paclitaxel, mice were sacrificed at 1 h following $^{99m}$Tc-EC-Guan injection (100 μCi/mouse, i.v.); immediately the body was frozen and fixed in carboxymethyl cellulose (4%), and further frozen on dry ice to solidify the block. The block was mounted onto a cryostat and cut into 100-μm coronal sections. Autoradiograms were viewed by a quantitative image analyzer.

### Statistical Analysis

Percent of injected dose per gram of tissue weight (%ID/g) and tumor/tissue ratios were presented as means and standard errors of means. To compare differences in %ID/g and tumor/tissue ratios between control and EC–conjugate groups, a Student's *t* test was used. Statistical significance was assigned if $p < 0.05$. All statistical computations were processed using Statview software 4.1 (Abacus, Berkeley, CA, USA).

**Table I.** Biodistribution of $^{99m}$Tc-EC in Breast Tumor-Bearing Rats

| | Percent of injected $^{99m}$Tc-EC dose per gram of tissue weight[a] | | |
|---|---|---|---|
| | 30 min | 2 h | 4 h |
| Blood | 0.273 ± 0.039 | 0.211 ± 0.001 | 0.149 ± 0.008 |
| Lung | 0.187 ± 0.029 | 0.144 ± 0.002 | 0.120 ± 0.012 |
| Liver | 0.367 ± 0.006 | 0.286 ± 0.073 | 0.234 ± 0.016 |
| Kidney | 8.991 ± 0.268 | 9.116 ± 0.053 | 7.834 ± 1.018 |
| Intestine | 0.787 ± 0.106 | 0.401 ± 0.093 | 0.103 ± 0.009 |
| Muscle | 0.043 ± 0.002 | 0.028 ± 0.009 | 0.019 ± 0.001 |
| Tumor | 0.149 ± 0.020 | 0.115 ± 0.002 | 0.096 ± 0.005 |
| Thyroid | 0.229 ± 0.118 | 0.106 ± 0.003 | 0.083 ± 0.005 |
| Stomach | 0.127 ± 0.106 | 0.037 ± 0.027 | 0.043 ± 0.014 |
| Tumor/Blood | 0.544 ± 0.004 | 0.546 ± 0.010 | 0.649 ± 0.005 |
| Tumor/Muscle | 3.414 ± 0.325 | 4.425 ± 0.397 | 5.093 ± 0.223 |

[a] Each rat was given 25 μCi of $^{99m}$ Tc-EC. Values shown represent the mean ± standard deviation from three animals at each time point.

**Table II.** Biodistribution of $^{99m}$Tc-EC-Guan in Breast Tumor Bearing Rats

| | Percent of injected $^{99m}$Tc-EC-Guan dose per gram of tissue weight[a] | | |
|---|---|---|---|
| | 30 min | 2 h | 4 h |
| Blood | 0.953 ± 0.113[b] | 0.421 ± 0.022[b] | 0.323 ± 0.028[b] |
| Lung | 0.683 ± 0.071[b] | 0.382 ± 0.071[b] | 0.239 ± 0.024[b] |
| Liver | 5.265 ± 0.681[b] | 6.718 ± 0.416[b] | 5.692 ± 0.153[b] |
| Kidney | 7.041 ± 0.682 | 7.637 ± 0.961 | 8.361 ± 1.070 |
| Intestine | 0.309 ± 0.084[b] | 0.155 ± 0.029[b] | 0.102 ± 0.009 |
| Muscle | 0.105 ± 0.014[b] | 0.042 ± 0.006[b] | 0.026 ± 0.001[b] |
| Tumor | 0.436 ± 0.019[b] | 0.267 ± 0.018[b] | 0.240 ± 0.032[b] |
| Thyroid | 0.448 ± 0.087 | 0.219 ± 0.020[b] | 0.114 ± 0.026 |
| Stomach | 0.301 ± 0.040 | 0.083 ± 0.035 | 0.052 ± 0.020 |
| Tumor/Blood | 0.457 ± 0.043 | 0.635 ± 0.036[b] | 0.736 ± 0.048 |
| Tumor/Muscle | 4.150 ± 0.473 | 6.409 ± 0.614[b] | 9.350 ± 0.307[b] |

[a] Values shown represent the mean ± SD from three animals at each time point.
[b] Significantly different ($p < 0.05$, *t*-test) compared to $^{99m}$ Tc-EC at the corresponding time interval.

## RESULTS

### Chemistry

Ethylenedicysteine was prepared in a two-step manner and yielded a pure L,L-EC form. It was conjugated to an amino analog of guanine under mild basic condition (pH 8.5). Although alternative structures such as EC conjugate to –OH group of penciclovir or EC conjugate to $NH_2$ at position 2 of guanine nucleus may occur, the reaction was conducted in aqueous condition. Thus, it is unlikely to form an ester conjugation. The amino ($NH_2$) at position 2 of guanine nucleus has a stable resonance and the alkyl $NH_2$ is more reactive than $NH_2$ at position 2; thus, we identified that EC was conjugated to the alkyl $NH_2$ group. Ethylenedicysteine-Guan was isolated using simple dialysis with molecule cut-off at 500. After dialysis, there was no dimeric EC species found

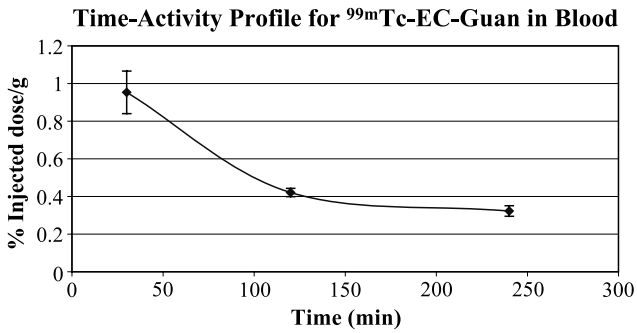


**Fig. 7.** Blood was collected from rats at 0.5, 2, and 4 h postinjection of $^{99m}$Tc-EC-Guan and measured for radioactivity. Biological half-life was determined to be approximately 74 min.

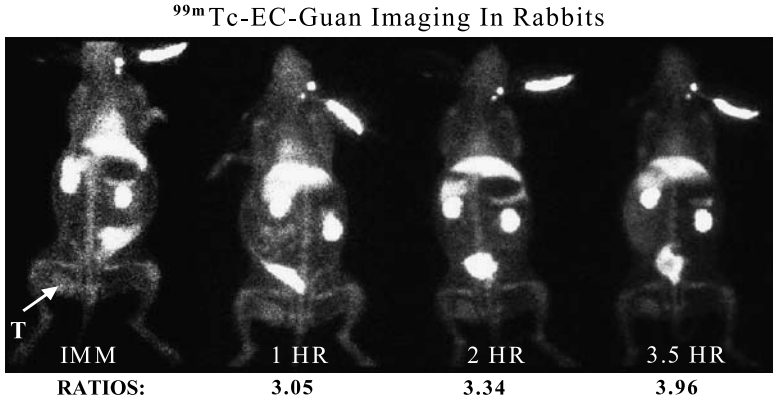


**Fig. 8.** Planar scintigraphy of $^{99m}$Tc-EC-Guan in VX2 tumor-bearing rabbits (1 mCi/rabbit, i.v. injection) demonstrated that tumor could be well-visualized (arrow) and an increased tumor/nontumor (opposite leg, muscle) ratios (3.1–4.0) were obtained at 1–3.5 h.

in the finished product. From radio-TLC analysis (Bioscan, Washington, DC, USA), the $R_f$ value and radiochemical purity were 0.8 and >97%, respectively.

### Cell Cycle Uptake Assays

Cell cycle uptake assays using lung tumor cells indicated that there was a high uptake of $^{99m}$Tc-EC-Guan, whereas $^{18}$F-FDG and $^{99m}$Tc-EC (control) had poor uptake (Fig. 2). The FACS analysis of $^{99m}$Tc-EC-Guan revealed that the uptake in S-phase was higher than in G2/M and G0/G1 phases. The findings suggest that $^{99m}$Tc-EC-Guan is involved in cell nuclei DNA synthesis.

### [$^3$H]Thymidine Incorporation Assay

Thymidine incorporation assays indicated that EC-Guan and glucose did not block cellular uptake of [$^3$H]thymidine, whereas FDG showed dose-dependent effects (Fig. 3). The findings suggest that EC-Guan and glucose interact with endogenous thymidine kinase, subsequently measuring the proliferative activity of the cell cycle; yet FDG had less involvement in cell nuclei activity.

### *In Vitro* Cellular Uptake of $^{99m}$Tc-EC-Guan

There was an increased uptake of $^{99m}$Tc-EC-Guan as a function of incubation time in the cancer cell lines tested (Figs. 4–6). Uptake of $^{99m}$Tc-EC as the control group was less that 0.1% at any time point. There is a twofold difference at 30 min, whereas there were no differences among HSV-tk gene, b-gal gene, and uninfected groups at 2 h incubation (Fig. 6). The data indicated that $^{99m}$Tc-EC-Guan, a cell cycle specific and an HSV-tk gene independent marker, could assess cellular proliferation.

### Biodistribution and Dosimetry of $^{99m}$Tc-EC-Guan in Tumor-Bearing Rats

Biodistribution of $^{99m}$Tc-EC and $^{99m}$Tc-EC-Guan in tumor bearing rats and mice is shown in Tables I and II. Blood samples was collected from rats at 0.5, 2, and 4 h postinjection of $^{99m}$Tc-EC-Guan and measured for radioactivity. Biological half-life was determined to be approximately 74 min (Fig. 7). Although tumor/blood and tumor/muscle count density ratios were increased as a function of time in $^{99m}$Tc-EC and $^{99m}$Tc-EC-Guan groups, accumulation of

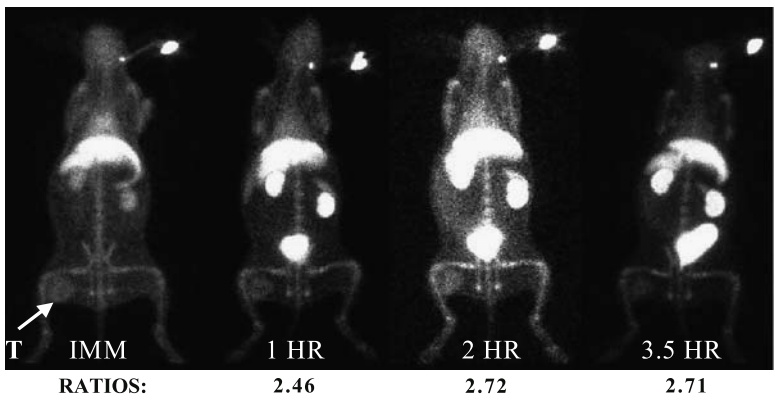


**Fig. 9.** Planar scintigraphy of $^{99m}$Tc-EC in VX2 tumor-bearing rabbits (1 mCi/rabbit, i.v. injection) showed that tumor/nontumor (opposite leg, muscle) ratios were 2.5–2.7 at 1–3.5 h.

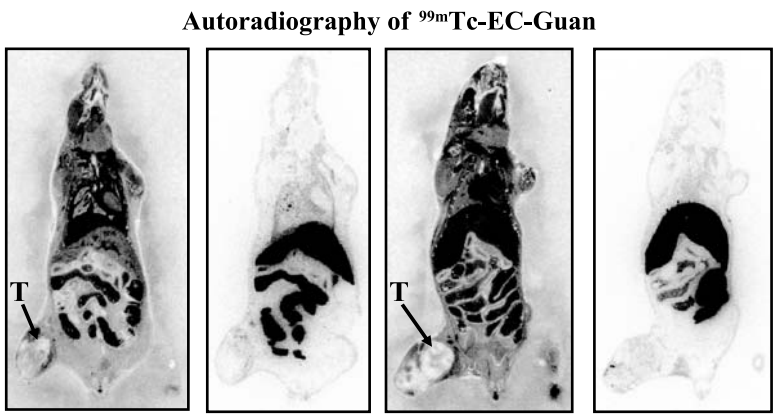


**Fig. 10.** Ovarian tumor-bearing nude mice were injected with 100 μCi of $^{99m}$Tc-EC-Guan pre- (left, panels 1 and 2) and post- (right, panels 3 and 4) paclitaxel treatment (60 mg/kg, i.v.), and sacrificed 60 min postinjection. Although different mice were used for evaluation of paclitaxel treatment response using autoradiographic technique, the tumor volume selected at baseline are very similar. Autoradiograms are shown in panels 1 and 3. The corresponding anatomical pictures are shown in panels 2 and 4. Sections were cut at 100 μm and exposed for 16 h. Arrow designates the tumor site. There was no enlargement of the tumor in the mouse treated with paclitaxel. The findings indicated the feasibility of using $^{99m}$Tc-EC-Guan to assess tumor growth.

$^{99m}$Tc-EC-Guan in tumors was significantly different from $^{99m}$Tc-EC at any time point ($p < 0.05$, $t$ test).

### Planar Scintigraphic Imaging

In gamma-scintigraphic imaging studies in tumor-bearing rabbits, tumor/muscle (T/M) ratios in $^{99m}$Tc-EC-Guan and $^{99m}$Tc-EC groups at 1–3.5 h post injection were 3.1–4.0 and 2.5–2.7, respectively (Figs. 8 and 9). Although tumor detection was observable in the leg, detection in the body cavity may be hampered by the background intensity of the internal organs. The $^{99m}$Tc-EC alone allowed detection although at a lower ratio. Increased T/M ratios were observed in the $^{99m}$Tc-EC-Guan group compared to the $^{99m}$Tc-EC group at the corresponding time interval.

### Autoradiography

Autoradiographic studies in ovarian tumor-bearing nude mice with $^{99m}$Tc-EC-Guan showed that tumor volume changes could be assessed at pre- and posttreatment with paclitaxel. Although different mice were used for evaluation of paclitaxel treatment response using autoradiographic technique, the tumor volume selected at baseline was very similar. There was no enlargement of the tumor in the mouse treated with paclitaxel (Fig. 10). The findings indicated the feasibility of using $^{99m}$Tc-EC-Guan to assess tumor growth.

## DISCUSSION

To develop novel or clinically used tracers, two types of chemistries are frequently used in the preparation of radiotracers: covalent and ionic. In covalent chemistry, either displacement or addition reactions are used to place an isotope in the molecule. The labeled product provides minimal structural alteration; however, the procedure may be lengthy, tedious, costly, and produce low yield. Isotopes commonly used in covalent chemistry include $^{18}$F, $^{123}$I, $^{131}$I, $^{75}$Br, $^{77}$Br, and $^{11}$C. In ionic chemistry, a chelator is required to trap metal isotopes. This type of chemistry is simple and produces high yield. The isotopes may be obtained from generators. Although ionic chemistry is attractive, the chemical properties may be altered due to addition of a chelator. We have previously reported that a series of EC–agent conjugates could target the tumor targets (21–28). Ethylenedicysteine is a small molecule and has been shown to be a stable chelator with $^{111}$In, $^{67/68}$Ga, and other metals (29). Here, we used 9-[4-hydroxy-3-(hydroxymethyl)butyl]guanine (penciclovir) as a target agent. Penciclovir and other guanine agents were used to assess reporter gene expression (7–10). Interestingly, our data revealed that conjugation of EC to penciclovir (EC-Guan) altered penciclovir affinity for assessing the efficiency of gene transfer. Our data showed that there was no difference in cellular uptake between transfected and uninfected tumor cells. Others have also shown that even a small modification in the sugar moiety of the pyrimidine analog can dramatically change the biological activity (30). Our hypothesis states that EC-Guan interacts with endogenous thymidine kinase, subsequently targeting S-phase of the cell cycle. The cellular uptake of $^{99m}$Tc-EC-Guan was shown to be S-phase-specific in sorted cells. Phosphorylation of $^{99m}$Tc-EC-Guan might have occurred in cytosol through various kinases. Subsequently, this agent was translocated to the cell nuclei as evidenced in thymidine incorporation assays. $^{99m}$Tc-EC-Guan overcomes the sensitivity deficiencies of HSV1-tk enzyme expression. $^{99m}$Tc-EC-Guan may be useful in assessing the endpoints of cancer therapy (e.g., cell proliferation).

Although FDG-PET imaging demonstrates the increased glucose consumption of malignant cells, problems with specificity for cell proliferation have led to the development of new PET tracers. 3′-Deoxy-3′-$^{18}$F-fluorothymidine ($^{18}$F-

FLT) is a new tracer that images cellular proliferation by entering the salvage pathway of DNA synthesis. Although FLT was shown to be a promising agent to assess cell proliferation, its DNA incorporation rate is low and its chemistry is complex (31). Deep-seated tumors in blood-rich organs may require significantly higher ratios for the assessment of proliferation. To enhance biological activity and increase chemical or metabolic stability, fluorine substitution at the C2′ position of the sugar moiety (arabino configuration) has been widely investigated in drug research (32,33). However, its chemistry is complex, involving several steps in the synthesis. To assess tumor growth, we selected guanine because it is involved in both mRNA and DNA pathways, unlike thymidine, which mainly involves DNA pathways. The biological half-life of $^{99m}$Tc-EC-Guan was determined to be approximately 74 min, which is three to four times longer than known purine- and pyrimidine-based agents (34).

Our preclinical data indicated that EC-Guan was involved in the cell cycle S-phase. Its simple chemistry also overcomes the complex chemistry of $^{18}$F-FLT. Although many other radiopharmaceuticals could be used for assessment of tumor proliferation and/or metabolic activity (3), the choice should be determined not only by the biological behavior of radiopharmaceuticals, but also by its ease of preparation.

## CONCLUSIONS

In summary, we have developed $^{99m}$Tc-EC-Guan, and our findings suggest that $^{99m}$Tc-EC-Guan incorporates into tumor cell DNA/RNA, which can be used as a predictor of tumor proliferative activity.

## ACKNOWLEDGMENTS

The authors wish to thank Eloise Daigle for her secretarial support. This work was supported in part by Cell>Point L.L.C (MDA LS01-212) and the John S. Dunn Foundation. The animal research and NMR facility was supported by M. D. Anderson Cancer Center (CORE) Grant NIH CA-16672.

## REFERENCES

1. K. Kubota, K. Ishiwata, R. Kubota, S. Yamada, M. Tada, T. Sato, and T. Ido. Tracer feasibility for monitoring tumor radiotherapy: a quadruple tracer study with fluorine-18-fluorodeoxyglucose or fluorine-18-fluorodeoxyuridine L-[methy1-$^{14}$C]methionine,[6-$^{3}$H]thymidine, and gallium-67. *J. Nucl. Med.* **32**:2118–2123 (1991).
2. J. Okada, K. Yoshihawa, M. Itami, K. Imaseki, K. Uno, J. Itami, J. Kuyama, A. Mikata, and N. Arimizu. Positron emission tomography using fluorine-18-fluorodeoxyglucose in malignant lymphoma: a comparison with proliferative activity. *J. Nucl. Med.* **33**:325–329 (1992).
3. K. Higashi, A. C. Clavo, and R. L. Wahl. Does FDG uptake measure proliferative activity of human cancer cells? *In vitro* comparison with DNA flow cytometry and tritiated thymidine uptake. *J. Nucl. Med.* **34**:414–419 (1992).
4. J. McConathy, L. Martarello, E. J. Malveaux, V. M. Camp, N. E. Simpson, C. P. Simpson, G. D. Bowers, Z. Zhang, J. J. Olson, and M. M. Goodman. Synthesis and evaluation of 2-amino-4-[(18)F]fluoro-2-methylbutanoic acid (FAMB): relationship of amino acid transport to tumor imaging properties of branched fluorinated amino acids. *Nucl. Med. Biol.* **30**:477–490 (2003).
5. P. L. Jager, B. E. Plaat, E. G. de Vries, W. M. Molenaar, W. Vaalburg, D. A. Piers, and H. J. Hoekstra. Imaging of soft-tissue tumors using L-3-[iodine-123]iodo-alpha-methyl-tyrosine single photon emission computed tomography: comparison with proliferative and mitotic activity, cellularity, and vascularity. *Clin. Cancer Res.* **6**:2252–2259 (2000).
6. J. G. Tjuvajev, M. Doubrovin, T. Akhurst, S. Cai, J. Balatoni, M. M. Alauddin, R. Finn, W. Bornmann, H. Thaler, P. S. Conti, and R. G. Blasberg. Comparison of radiolabeled nucleoside probes (FIAU, FHBG, and FHPG) for PET imaging of HSV1-tk gene expression. *J. Nucl. Med.* **43**:1072–1083 (2002).
7. M. Namavari, J. R. Barrio, T. Toyokuni, S. S. Gambhir, S. R. Cherry, H. R. Herschman, M. E. Phelps, and N. Satyamurthy. Synthesis of 8-[$^{18}$F]fluoroguanine derivatives: *in vivo* probes for imaging gene expression with positron emission tomography. *Nucl. Med. Biol.* **27**:157–162 (2000).
8. S. S. Gambhir, E. Bauer, M. E. Black, Q. Liang, M. S. Kokoris, J. R. Barrio, M. Iyer, M. Namavari, M. E. Phelps, and H. R. Herschman. A mutant herpes simplex virus type 1 thymidine kinase reporter gene shows improved sensitivity for imaging reporter gene expression with positron emission tomography. *Proc. Natl. Acad. Sci. USA* **97**:2785–2790 (2000).
9. M. Iyer, J. R. Barrio, M. Namavari, E. Bauer, N. Satyamurthy, K. Nguyen, T. Toyokuni, M. E. Phelps, H. R. Herschman, and S. S. Gambhir. 8-[18F]Fluoropenciclovir: an improved reporter probe for imaging HSV1-tk reporter gene expression *in vivo* using PET. *J. Nucl. Med.* **42**:96–105 (2001).
10. M. M. Alauddin and P. S. Conti. Synthesis and preliminary evaluation of 9-(4-[$^{18}$F]-fluoro-3-hydroxymethylbutyl)guanine ([$^{18}$F]FHBG): a new potential imaging agent for viral infection and gene therapy using PET. *Nucl. Med. Biol.* **25**:175–180 (1998).
11. H. Barthel, M. Perumal, J. Latigo, Q. He, F. Brady, S. K. Luthra, P. M. Price, and E. O. Aboagye. The uptake of 3′-deoxy-3′-[($^{18}$)F]fluorothymidine into L5178Y tumours *in vivo* is dependent on thymidine kinase 1 protein levels. *Eur. J. Nucl. Med. Mol. Imaging* **32**:257–263 (2005).
12. P. Goethals, M. V. Eijkeren, W. Lodewyck, and R. Dams. Measurement of [methyl-carbon-11]thymidine and its metabolites in head and neck tumors. *J. Nucl. Med.* **36**:880–882 (1995).
13. J. Tjuvajev, H. A. Macapinlac, F. Daghighian, A. M. Scott, J. Z. Ginos, R. D. Finn, P. Kothari, R. Desai, J. Zhang, B. Beattie, M. Graham, S. M. Larson, and R. G. Blasberg. Imaging of brain tumor proliferative activity with iodine-131-iododeoxyuridine. *J. Nucl. Med.* **35**:407–1417 (1994).
14. Y. Abe, H. Fukuda, K. Ishiwata, S. Yoshioka, K. Yamada, S. Endo, K. Kubota, T. Sato, T. Matsuzawa, T. Takahashi, and T. Ido. Studies on $^{18}$F-labeled pyrimidines tumor uptakes of $_{18}$F-5-Flourouracil, $^{18}$F-5-Flourouridine, and $^{18}$F-5-Flourodeoxyuridine in animals. *Eur. J. Nucl. Med.* **8**:258–261 (1983).
15. C. G. Kim, D. J. Yang, E. E. Kim, A. Cherif, L. R. Kuang, C. Li, W. Tansey, C. W. Liu, S. C. Li, S. Wallace, and D. A. Podoloff. Assessment of tumor cell proliferation using [$^{18}$F]fluorodeoxyadenosine and [$^{18}$F]fluoroethyluracil. *J. Pharm. Sci.* **85**:339–344 (1996).
16. K. Ohtsuki, K. Akashi, Y. Aoka, F. G. Blankenberg, S. Kopiwoda, J. F. Tait, and H. W. Strauss. Technetium-$^{99m}$ HYNIC-annexin V: a potential radiopharmaceutical for the *in-vivo* detection of apoptosis. *Eur. J. Nucl. Med.* **26**(10): 1251–1258 (1999).
17. C. G. Van Nerom, G. M. Bormans, M. J. De Roo, and A. M. Verbruggen. First experience in healthy volunteers with technetium-$^{99m}$ L,L-ethylenedicysteine, a new renal imaging agent. *Eur. J. Nucl. Med.* **20**:738–746 (1993).
18. E. P. Canet, C. Casali, A. Desenfant, M. Y. An, C. Corot, J. F. Obadia, D. Revel, and M. F. Janier. Kinetic characterization of CMD-A2-Gd-DOTA as an intravascular contrast agent for myocardial perfusion measurement with MRI. *Magn. Reson. Med.* **43**:403–409 (2000).
19. H. C. Wu, C. H. Chang, M. M. Lai, C. C. Lin, C. C. Lee, and A. Kao. Using Tc-$^{99m}$ DMSA renal cortex scan to detect renal damage in women with type 2 diabetes. *J. Diabet. Complicat.* **17**:297–300 (2003).

20. Y. Li, A. E. Martell, R. D. Hancock, J. H. Reibenspies, C. J. Anderson, and M. J. Welch. *N,N′*-Ethylenedicysteine (EC) and its metal complexes: synthesis, characterization crystal structures, and equilibrium constants. *Inorg. Chem.* **35**(2):404–414 (1996).
21. S. Ilgan, D. J. Yang, T. Higuchi, F. Zareneyrizi, H. Bayhan, D.-F. Yu, E. E. Kim, and D. A. Podoloff. $^{99m}$Tc-Ethylenedicysteinefolate: a new tumor imaging agent. Synthesis, labeling and evaluation in animals. *Cancer Biother. Radiopharm.* **13**:427–435 (1998).
22. F. Zareneyrizi, D. J. Yang, C.-S. Oh, S. Ilgan, D.-F. Yu, W. Tansey, C.-W. Liu, E. E. Kim, and D. A. Podoloff. Synthesis of $^{99m}$Tc-ethylenedicysteine–colchicine for evaluation of antiangiogenic effects. *Anti-cancer Drugs* **10**:685–692 (1999).
23. D. J. Yang, S. Ilgan, T. Higuchi, F. Zareneyrizi, C. S. Oh, C.-W. Liu, E. E. Kim, and D. A. Podoloff. Noninvasive assessment of tumor hypoxia with $^{99m}$Tc-labeled metronidazole. *Pharm. Res.* **16**:743–750 (1999).
24. D. J. Yang, A. Azhdarinia, P. Wu, D.-F. Yu, W. Tansey, S. Kohanim, E. E. Kim, and D. A. Podoloff. *In vivo* and *in vitro* measurement of apoptosis in breast cancer cells using $^{99m}$Tc-EC-annexin V. *Cancer Biother. Radiopharm.* **16**:73–84 (2001).
25. D. J. Yang, K.-D. Kim, N. R. Schechter, D.-F. Yu, P. Wu, A. Azhdarinia, J. S. Roach, S. Kohanim, K. Ozaki, W. E. Fogler, J. L. Bryant, R. S. Herbst, J. Abbruzzes, E. E. Kim, and D. A. Podoloff. Assessment of antiangiogenic effect using $^{99m}$Tc-EC-endostatin. *Cancer Biother. Radiopharm.* **17**:233–246 (2002).
26. N. R. Schechter, D. J. Yang, A. Azhdarinia, S. Kohanim, R. Wendt III, C. S. Oh, M. Hu, D. F. Yu, J. Bryant, K. K. Ang, K. M. Forster, E. E. Kim, and D. A. Podoloff. Assessment of epidermal growth factor receptor with $^{99m}$Tc-ethylenedicysteine-C225 monoclonal antibody. *Anti-cancer Drugs* **14**:49–56 (2003).
27. D. J. Yang, C. G. Kim, N. R. Schechter, A. Azhdarinia, D. F. Yu, C. S. Oh, J. L. Bryant, J. J. Won, E. E. Kim, and D. A. Podoloff. Imaging with $^{99m}$Tc ECDG targeted at the multifunctional glucose transport system: feasibility study with rodents. *Radiology* **226**:465–473 (2003).
28. H. C. Song, H. S. Bom, K. H. Cho, B. C. Kim, J. J. Seo, C. G. Kim, D. J. Yang, and E. E. Kim. Prognostication of recovery in patients with acute ischemic stroke through the use of brain SPECT with $^{99m}$Tc-labeled metronidazole. *Stroke* **34**:982–986 (2003).
29. Y. Li, A. E. Martell, R. D. Hancock, J. H. Reibenspies, C. J. Anderson, and M. J. Welch. *N,N′*-Ethylenedi-L-cysteine (EC) and its metal complexes: synthesis, characterization crystal structures, and equilibrium constants. *Inorg. Chem.* **35**(2):404–414 (1996).
30. H. Griengle, E. Wanek, W. Schwarz, W. Streicher, B. Rosenwirth, and E. D. Clercq. 2′-Fluorinated arabinonucleosides of 5-(2-haloalkyl)uracil: synthesis and antiviral activity. *J. Med. Chem.* **30**: 1199–1204 (1987).
31. D. L. Francis, D. Visvikis, D. C. Costa, T. H. Arulampalam, C. Townsend, S. K. Luthra, I. Taylor, and P. J. Ell. Potential impact of [$^{18}$F]3′-deoxy-3′-fluorothymidine *versus* [$^{18}$F]fluoro-2-deoxy-D-glucose in positron emission tomography for colorectal cancer. *Eur. J. Nucl. Med. Mol. Imaging* **30**:988–994 (2003).
32. S. Uesugi, T. Kaneyasu, and M. Ikehara. Synthesis and properties of ApU analogues containing 2′-halo-2′-deoxyadenosine. Effect of 2′ substituents on oligonucleotide conformation. *Biochemistry* **21**:5870–5877 (1982).
33. L. Malspeis, M. R. Grever, A. E. Staubus, and D. Young. Pharmacokinetics of 9-B-arabinofuranosy1-2-fluoroadenine in cancer patients during the phase I clinical investigation of fludarabine phosphate. *Semin. Oncol.* **17**:18–32 (1990).
34. P. Khalili, E. Naimi, E. E. Knaus, and L. I. Wiebe. Pharmacokinetics and metabolism of the novel synthetic C-nucleoside, 1-(2-deoxy-beta-D-ribofuranosyl)-2,4-difluoro-5-iodobenzene: a potential mimic of 5-iodo-2′-deoxyuridine. *Biopharm. Drug Dispos.* **23**(3):105–113 (2002).